A Direct Determination of the Magnetic Moment of the Protons in Units of the Nuclear Magneton*†

C. D. JEFFRIES
Stanford University, Stanford, California††

(Received November 10, 1950)

A direct measurement of the proton magnetic moment in units of the nuclear magneton has been made, using the method of Alvarez and Bloch. The experiment consists of comparison of the nuclear magnetic resonance frequency of protons with the orbital frequency of protons revolving in the same homogeneous field. The resonance frequency of protons in water has been measured by the method of nuclear induction; the orbital frequency has been measured by a special device: a small decelerating cyclotron operated at an odd multiple of the fundamental cyclotron frequency.

The device has been operated in a field of about 5300 gauss at all odd multiples from the first to the eleventh, with a corresponding range of the dee frequency between 8.1 and 89 Mc/sec. As expected, the sharpness of the cyclotron resonance was observed to greatly increase at the higher multiples; besides this advantage for obtaining high accuracy, the comparison of the results at different multiples also furnished an important check on the reliability of the measurements.

An approximate theory for the shape of the cyclotron resonance curves has been developed, and its qualitative agreement with the observations has been established. The perturbing effects of extraneous electric and magnetic fields have been investigated, both theoretically and experimentally, and found to be negligible. With the smallest relative half-width of resonance about 1/10,000, which was observed at the higher multiples, and guided by the interpretation of the resonance shape, the magnetic moment of the proton has been found to be 2.7924 ± 0.0002 nuclear magnetons.

I. INTRODUCTION

THROUGH the development of new experimental methods it has been possible, in recent years, to achieve relative measurements of nuclear magnetic moments, with high accuracy. They are based on the comparison of resonance frequencies, and the magnetic moment of the proton has been chosen as the common standard to which other moments are referred. This choice has been motivated by convenience as well as by the basic significance of the proton moment. Nevertheless, there remains the problem of measuring the proton moment μ_p itself with comparable accuracy in terms of the natural unit of nuclear magnetic moments, the "nuclear magneton" $\mu_n=eh/4\pi Mc=\mu_B m/M$ (e=elementary charge, c=velocity of light, h=Planck's constant, M=mass of proton, m=mass of electron, μ_B=Bohr magneton).

Starting with the first measurement by Stern and Frisch,[1] the proton moment has been redetermined repeatedly with increasing accuracy by atomic and molecular beam experiments.[2–4] In these experiments, however, it is not directly the ratio μ_p/μ_n which is measured, but μ_p is either obtained in absolute units or in units of the magnetic moment of the electron. Applying the necessary radiative corrections to the latter, the most accurate value obtained in this way was given by Taub and Kusch[5] as $\mu_p=2.7935\mu_n$.

A method for determining directly nuclear magnetic moments in units of the nuclear magneton was described several years ago by Alvarez and Bloch;[6] it is based on the comparison of the nuclear resonance frequency with the orbital frequency of protons revolving in a magnetic field. Through the recent developments, which allow convenient and precise measurements of nuclear resonance frequencies,[7,8] this method is now capable of high accuracy. By a modification, consisting in the comparison of the nuclear resonance frequency of protons with the orbital frequency of *electrons*, Purcell and Gardner[9] have thus been able to obtain a direct determination of the proton magnetic moment in units of the *Bohr magneton*.

Correspondingly, it is the aim of the experiment reported here, and briefly published earlier,[10] to compare the proton resonance frequency, observed by nuclear induction, with the orbital frequency of *protons* in the same magnetic field and thus to obtain directly the proton magnetic moment in units of the *nuclear magneton*. In conjunction with the measurement of Purcell and Gardner it can also be considered as a new method for determining the mass ratio of the proton to the electron.

While this experiment has been in progress, a similar one based on the same principle has been carried out by Hipple, Sommer, and Thomas[11] to determine the value of the Faraday. In their apparatus, the "omegatron," protons are accelerated by an essentially homogeneous oscillating electric field, and they are trapped in an

* This paper is based on a dissertation submitted to the Department of Physics and the Committee on Graduate Study of Stanford University in partial fulfillment of the requirements for the degree of Doctor of Philosophy.

† Assisted by the joint program of the AEC and ONR.

†† Present address: Physikalisches Institut der Universität Zürich, Zürich, Switzerland.

[1] R. Frisch and O. Stern, Z. Physik **85**, 4 (1933).

[2] Rabi, Kellogg, and Zacharias, Phys. Rev. **46**, 157, 163 (1934).

[3] S. Millman and P. Kusch, Phys. Rev. **60**, 91 (1941).

[4] Kellogg, Rabi, Ramsey, and Zacharias, Phys. Rev. **56**, 728 (1939).

[5] H. Taub and P. Kusch, Phys. Rev. **75**, 1481 (1949).

[6] L. W. Alvarez and F. Bloch, Phys. Rev. **57**, 111 (1940).

[7] Purcell, Torrey, and Pound, Phys. Rev. **69**, 37 (1946); Bloembergen, Purcell, and Pound, Phys. Rev. **73**, 679 (1948).

[8] Bloch, Hansen, and Packard, Phys. Rev. **69**, 127 (1946); and Phys. Rev. **70**, 474 (1946); F. Bloch, Phys. Rev. **70**, 460 (1946).

[9] J. H. Gardner and E. M. Purcell, Phys. Rev. **76**, 1262 (1949).

[10] F. Bloch and C. D. Jeffries, Phys. Rev. **80**, 305 (1950).

[11] Hipple, Sommer, and Thomas, Phys. Rev. **76**, 1877 (1949) and Phys. Rev. **80**, 487 (1950).

electric dc potential. Compared with ours, this arrangement has the advantage that it avoids the difficulties of injection; also, up to the present time, it has yielded resonance widths about 3 times smaller than those obtained by our device. On the other hand, the omegatron involves certain perturbations due to space charges and it precludes the feature of operation at higher multiples of the orbital frequency, of which our decelerating cyclotron is capable. For these reasons, as well as for the mutual checking of results obtained by the two different methods, it seemed to us well worth while to develop our technique further.

II. METHOD

As suggested by Alvarez and Bloch,[6] the problem of measuring μ_p/μ_n can be solved by a method of high inherent accuracy based on the measurement of a frequency ratio; by observing both the nuclear resonance frequency ν_N of protons in a magnetic field H' and the orbital frequency ν_R of protons revolving in a magnetic field H, we have

$$\nu_N=2\mu_p H'/h, \quad \nu_R=eH/2\pi Mc \tag{1}$$

and, therefore,

$$H\nu_N/H'\nu_R=\mu_p/(eh/4\pi Mc)=\mu_p/\mu_n. \tag{2}$$

Thus, by performing both experiments in the same homogeneous magnetic field, we may take $H=H'$ in Eq. (2) and μ_p/μ_n is then given directly as the ratio of two frequencies to an accuracy determined, in principle, by the bandwidths of the two resonance phenomena involved; i.e., by the number of coherent cycles in an observation.

We have used the method of nuclear induction both to measure ν_N to within a few parts in 10^5 and to make the magnetic field homogeneous to comparable accuracy. The accuracy of the present experiment hinges then on the determination of ν_R, which we have measured to about one part in 10^4. To obtain this accuracy it is not possible to determine ν_R by measuring the resonant frequency of a conventional accelerating cyclotron because the resonance bandwidth is broadened too much by the magnetic focusing, by a limitation in the number of revolutions due to gas scattering, and by relativistic mass variation. Actually, to be able to apply Eq. (2) with high accuracy, the following requirements are necessary:

(1) The field H must be highly homogeneous over the entire proton orbit. The possibility of magnetic focusing is thus excluded, and some other means must be provided to prevent loss of the protons after many revolutions. We have utilized the electric phase focusing property of cyclotron dees, while in the "omegatron,"[11] loss of protons is prevented by "trapping" them in an electric potential well.

(2) The gas pressure must be sufficiently low in order that collisions do not seriously limit the number of revolutions. This was achieved by operating a cyclotron in an inverse or decelerating fashion, in which the protons are formed in an external arc-source and brought into the dees through several stages of differential pumping—thus maintaining a low pressure in the dee cavity. Essentially, the protons traverse a conventional cyclotron trajectory in the backward direction and are detected by a probe near the center of the dees. This arrangement introduces the problems of injection, but it has other important advantages which will be discussed shortly.

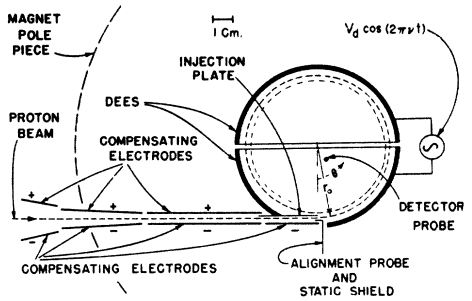

FIG. 1. Schematic arrangement of the decelerating cyclotron. Protons are injected into the dees at a radius r_0 and are decelerated by the dee voltage $V_d \cos(2\pi\nu t)$, where $\nu \cong n\nu_R = neH/2\pi Mc$ and n is an odd integer.

(3) The relativistic mass variation of a proton throughout its orbit must be negligible. This limits the proton energy eV to the order of magnitude of 10^4 electron volts, where the mass variation is $\Delta M/M \cong eV/Mc^2 \cong 10^{-5}$. Gas scattering is greater here than at higher energies; on the other hand, the radius of the orbit is conveniently small, which is a practical advantage for having the magnetic field homogeneous over its extension.

(4) Besides the above requirements it is important for high precision that perturbations of the frequency ν_R, due to extraneous electric and magnetic fields, be very small; this problem will be discussed later.

Guided by the above considerations we have constructed a small decelerating cyclotron as shown schematically in Fig. 1. The dees are 4.25 cm in radius, 1.65 cm wide, and are in a homogeneous field of about 5300 gauss, provided by a magnet with pole pieces of 13 cm radius. A beam of protons with energy $eV_0=2\times10^4$ electron volts is continuously injected tangentially into the dees, and resonance is determined by observing the frequency of the applied sinusoidal dee voltage at which the protons spiral sufficiently inward to strike a detector probe near the center of the dees. An incoming proton is directed along a straight path towards the dee periphery by means of a compensating field E_0, which compensates the Lorentz force on the proton and is provided by suitable compensating electrodes (Fig. 1). Without this compensation a proton entering from the outside into the gap of the magnet would be deflected away by the fringing field; the compensation must be effective up to the end of the injection plate (Fig. 1), where there is a transition from the straight line path to a spiral inside the dees.

This transition raises the fundamental problem of injection into an almost stable orbit, and this difficulty is, in our arrangement, expressed by two requirements: (1) that the proton orbit be a finely spaced spiral in order that a large number of revolutions can take place; (2) that the orbit be sufficiently coarsely spaced initially to afford a transition from a straight line path to a circular path, such that an entering proton clears the finite thickness d of the injection plate (Fig. 1) which shields the dee cavity from the field E_0. With an initial radius r_0 and energy eV_0 a proton must, in the first revolution, lose energy by an amount $eV=2eV_0d/r_0$; otherwise it will strike the injection plate and be lost. This limits the minimum amplitude of the dee voltage to $V_c=V_0d/r_0$. Because of construction difficulties, the smallest practical value of d/r_0 is about 10^{-2}. Therefore, the amplitude of the dee voltage must be about one percent of the initial voltage, which would seem to allow only about $N=V_0/2V_c=50$ revolutions with a corresponding resonance bandwidth[12] of about $1/2\pi N=1/300$.

We have solved the injection problem and actually achieved a very considerable reduction in the resonance bandwidth, and a corresponding gain in accuracy, by extending the operation of the cyclotron from the frequency ν_R of Eq. (1) to a frequency $n\nu_R$, where $n=3$, 5, 7, 9, or 11. The reduction in bandwidth is due to two circumstances; in the first place, operation of the dees at the nth multiple of ν_R will, for a given number of revolutions of a proton, reduce the observed resonance bandwidth by a factor n, since resonance conditions require a proportionally more critical timing between the dee oscillation and the rotation of the proton. In the second place, transit time effects permit an increase in the number of revolutions required for a proton to reach the probe at a given position. In fact, as the spiral orbit of a proton shrinks, it travels ever more slowly through the dee gap, so that the net decelerating action of the oscillating dee field during transit is more and more reduced. This effect is evidently the more pronounced the smaller the radius and the higher the dee frequency. The proton thus approaches the detector probe in an increasingly finely spaced spiral, which in our arrangement may easily contain 500 revolutions. The practical upper frequency limit is reached when the transit time effect becomes appreciable even at the initial radius r_0, consequently requiring a higher dee voltage for injection. Because of this limitation and also because of decreased focusing action for large n, we have been able to operate the present apparatus only up to the 11th multiple of ν_R, where we have observed resonance bandwidths of about one part in 10^4. However, except for increased technical difficulties, there is no reason why, in an apparatus of modified design, the method cannot be extended to appreciably higher multiple frequencies and correspondingly greater accuracies.

It should be pointed out that the transit time effect, which is advantageous for our experiment, actually prevents multiple frequency operation of an accelerating cyclotron where the protons are introduced at zero radius, so that dee fields at a multiple of the resonance frequency ν_R are ineffective in starting the protons into a spiral orbit.

Without actually carrying them out, we have also considered two alternative injection schemes which do not involve multiple frequencies: (1) If the dee voltage is kept at a very low voltage V' and at a frequency near ν_R, the occasional application of a pulse of approximate duration $1/\nu_R$ and with an amplitude $V>V_0d/r_0$ will inject protons and allow them to spiral down to the detector probe in a large number of revolutions. This will allow resonance bandwidths of the order of magnitude of $V'/\pi V_0$, which in principle can be made as small as other factors, such as decrease of focusing, will allow. The main disadvantage of this scheme is that the duty cycle of the proton current and, correspondingly, the magnitude of the detector probe current suffer a reduction proportional to the number of revolutions in the orbit. (2) The dees may be separated into two concentric parts: an outer split ring driven at relatively high voltages to allow injection, and a pair of inner dees at low voltage to allow many revolutions to take place. Apart from its technical difficulty, the disadvantage of this scheme lies in the complicated analysis of the orbits in the transition region.

A. Analysis of Decelerating Cyclotron

It is essential for a precise measurement like the one presented here that, beyond the qualitative aspects, the principal features be understood in a quantitative manner, so that proper functioning of the apparatus and correct interpretation of the results may be obtained. In our experiment it is particularly important to analyse the motion of the protons and thereby to gain insight into the shape of the observed resonance curves. No attempt will be made to give a rigorous solution to the problem of the cyclotron motion of a particle in a pair of dees. Instead, a number of approximations will be made which are more or less justified in a theory which merely purports to analyse the principal features and determine the resonance frequency to within about $\frac{1}{3}$ of the resonance bandwidth.

First, we approximate the dees by a two dimensional set of infinite plates shown in cross section in Fig. 2. This approximation neglects the end effects due to the side walls of the dees; it is assumed further, and is well justified by the actual dimensions of our apparatus, that the gap separating the two dees is small compared to the dee width b. Secondly, we neglect the curving of the orbits due to the field H during the transition of the protons from one dee into the other. This means that b

[12] It is shown later that the resonance bandwidth is about $1/2\pi N$, where N is the number of revolutions at exact resonance of a proton crossing the gap at the instant of maximum dee voltage.

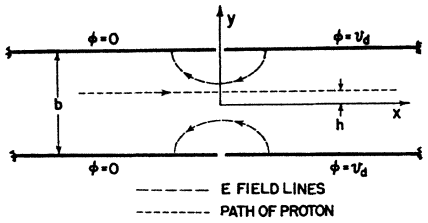

FIG. 2. Cross section of the electrode configuration used in approximating the dees in the calculations. The gap separating the dees is taken to be zero. The field H is in the y direction.

is considered to be sufficiently small compared to the radius of the orbit.[13]

Consider the effect of the electric field on a proton in transit through the plates in the x-direction with an energy very large compared to the dee voltage v_d in which case the path may be approximated by a straight line $y=h$. The lens focusing action due to the change in the proton velocity will be negligible. However, if v_d varies sinusoidally with time as the proton crosses the gap, it will be subject to phase focusing; i.e., it will receive a net transverse momentum either toward or away from the median plane, depending on the phase of the voltage. v_d must be positive for deceleration, and a proton will be focused if v_d is increasing in time when it passes the point $x=0$, and defocused if v_d is decreasing. The converse is true in a conventional accelerating cyclotron in which v_d is negative.

As shown in Appendix A, the approximate radial and transverse motion of a proton in dees of width b and radius R is given for $b \ll r < (\mathrm{R}-b)$ by the differential equations:

$$\frac{V_0}{r_0^2}\frac{dr}{dN} = -\frac{V_d}{r}\frac{\cosh(ny/r)}{\cosh(nb/2r)}\cos\delta, \tag{3}$$

$$\frac{M\pi\nu^2}{n^2}\frac{d^2y}{dN^2} = \frac{eV_d}{r}\frac{\sinh(ny/r)}{\cosh(nb/2r)}\sin\delta, \tag{4}$$

where r=radius of the proton orbit, y=displacement from the median plane of the dees, N=number of revolutions, V_d=amplitude of dee voltage, ν=frequency of dee voltage, n=an odd integer $\cong\nu/\nu_R$, δ=phase of dee voltage when the proton is midway between the two dees, and eV_0=proton energy at the radius r_0. δ may be expressed as a function of N and $\Delta\nu=\nu-n\nu_R$, so that

$$\begin{matrix}\sin\\ \cos\end{matrix}\left[\delta\right] = \begin{matrix}\sin\\ \cos\end{matrix}\left[\delta_0+(2\pi N\Delta\nu/\nu_R)\right], \tag{5}$$

where δ_0 is the initial value of δ at $N=0$.

From the form of Eq. (4) it is evident that the transverse motion is either concave or convex toward the median plane, depending on the sign of $\sin\delta$; i.e., there is phase focusing for negative $\sin\delta$ and defocusing for positive $\sin\delta$. In the case of focusing, the motion consists of oscillations about the median plane, which are sinusoidal for small amplitudes, i.e., for $ny \ll r$. Under typical conditions of this experiment the frequency of the transverse oscillation is small compared to ν_R.

Since we are interested in orbits containing many revolutions, protons for which $\sin\delta$ is positive even during a small portion of the orbit are defocused enough to strike the dees and do not reach the detector probe. The probe current is therefore almost entirely due to protons for which $\sin\delta$ is always negative and for which the amplitude of transverse oscillation remains less than $b/2$. The exact analysis of the transverse oscillation is a complex problem, the solution of which is not essential for our present purpose and will not be attempted. It can be stated, however, that the amplitude of oscillation is the greater, the larger the initial transverse proton velocity, the smaller $\sin\delta$, and the smaller the dee voltage. It can be seen further from Eq. (4) that for small values of y and large values of r/b, the focusing action starts to improve for increasing n, but becomes less effective if n becomes either too large or r too small. For $n=9$ or 11, and for the actual dimensions used in the present experiment, the focusing action continuously decreases with decreasing radius.

In the special case of exact resonance for protons in the median plane, i.e., for $\Delta\nu=0$, $y=0$, a solution of the radial motion can be obtained easily by integration of Eq. (3). This is done in Appendix A, where we have calculated for various values of n the number of revolutions N_0 necessary for a proton with initial radius r_0 to reach radius r, assuming that the phase δ is always zero, i.e., that the proton always crosses the dee gap when the voltage is at its maximum; this will be the case if the initial phase δ_0 is zero and the dee voltage is at the exact resonance frequency $n\nu_R$. With the radius of the dees only 0.4 cm larger than the initial radius $r_0=3.85$ cm, the neglect of the end effects made in this calculation is not strictly justified. In the beginning of the orbit, i.e., for r close to r_0, the side walls of the dees produce a shielding effect near the gap, and this will somewhat reduce N_0 from the values shown in Fig. 3. Nevertheless, this graph clearly shows the transit time effect; the higher the value of n, the more rapidly N_0 increases with decreasing radius.

For protons in the median plane it is possible to calculate the approximate shape of the resonance curve, i.e., the detector probe current as a function of the dee frequency ν near the resonance frequency $n\nu_R$. Although the results cannot be applied rigorously to the observed curves, they serve as a useful guide in the proper determination of the dee frequency at which exact resonance occurs.

Both the magnitude and the frequency dependence of the probe current are functions of the dee voltage. As was explained earlier in this section, no protons will be injected into the dees unless the dee voltage has an

[13] Our approach to the problem is similar to that of R. Wilson [Phys. Rev. **53**, 408 (1938)] and of M. Rose [Phys. Rev. **53**, 392 (1938)] in their analyses of an accelerating cyclotron.

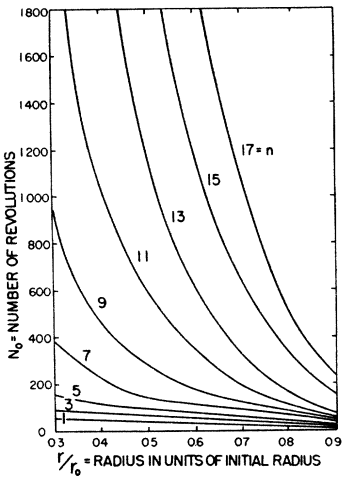

FIG. 3. The number of revolutions N_0 [Eq. (9A), Appendix A] which a proton in the median plane must make, starting from the radius r_0, in order to reach a radius r with a dee voltage $V_d=200$ volts peak at a frequency $n\nu_R$. The rapid increase in N_0 with decreasing radius for large n is due to the transit time effect. The phase δ is taken to be always zero, i.e., the proton encounters the peak dee voltage each time it crosses the dee gap. The constants have been chosen to correspond to the present experiment: $V_0=20$ kilovolts, $r_0=3.8$ cm, $b=1.65$ cm. N_0 may be calculated for any other dee voltage by using the relation $N_0 \propto 1/V_d$.

amplitude V_d at least as great as V_c, the cut-off value necessary for a proton to just clear the injection plate after one revolution. For $V_d=V_c$ only those protons immediately adjacent to the injection plate will enter; furthermore, they must pass through the dee gap when the voltage is at its maximum, i.e., their initial phase must be $\delta_0=0$.

If, for the moment, any focusing or defocusing action is disregarded, a proton will reach the detector probe at a radius r provided that the dee frequency ν is sufficiently near the resonance frequency $n\nu_R$ so that the phase δ remains within the values $-\pi/2$ and $+\pi/2$; i.e., the spiral orbit must continue to shrink by deceleration and must not start to expand by acceleration before the detector probe is reached. In the limiting case $V_d=V_c$, a vanishingly small probe current could be expected with a uniform and symmetric distribution around the frequency $n\nu_R$; the relative half width of this rectangular resonance curve is shown in Appendix B to be

$$\Delta\nu^*/n\nu_R=1/2\pi nN_0. \tag{6}$$

The preceding disregard of focusing and defocusing effects is, however, quite unrealistic. Even protons moving very closely in the median plane will rapidly be lost as soon as defocusing occurs, i.e., essentially as soon as the phase δ becomes positive, whereas for negative values of δ and consequent focusing, the protons will indeed reach the probe if the dee frequency is sufficiently near the resonance frequency. For $V_d=V_c$, the initial phase δ_0 is zero, and the phase δ becomes positive for $\Delta\nu=\nu-n\nu_R>0$; this requires that the previously discussed symmetric resonance curve be replaced by one whose total width is given by Eq. (6) and which lies entirely on the lower frequency side of resonance.

The next refinement is obtained by considering dee voltages V_d appreciably greater than V_c, in which case finite probe currents are obtained, since even entering protons not immediately adjacent to the injection plate will clear it after the first revolution; however, the initial phase angle δ_0 is now not required to be zero. Resonance curves are calculated in Appendix B and plotted in Fig. 4 for this case, still assuming that the focusing condition $-\pi/2<\delta<0$ is necessary and sufficient for a proton to reach the probe. The discontinuities in the slope are due to this assumption; a more detailed and rather complex analysis of the transverse motion would be necessary to avoid this assumption and to obtain continuous curves which, of course, are observed experimentally.

The plots in Fig. 4 are given for various dee voltages; the current amplitudes have been normalized to unity, and the widths are given in units of $\Delta\nu_c^*$, which is defined by Eq. (6) for a dee voltage of V_c. If the obvious discontinuities in these curves are smoothed out, they agree qualitatively with the experimentally observed resonance curves—the chief discrepancy being that, for the higher values of n, the experimental curves are somewhat wider. This discrepancy arises because Fig. 4 is based on the assumption that the protons stay very nearly in the median plane. This is not a realistic assumption, particularly at the higher multiple frequencies, where the focusing action decreases and the protons oscillate with appreciable amplitude about the median plane. As is evident from the factor $\cosh(ny/r)$ of Eq. (3), this means that these protons take fewer revolutions to reach the detector probe than do those in the median plane, with the result that the resonance is correspondingly broadened.

Although the previous analysis is not sufficient for an exact calculation of resonance curves, it contains, nevertheless, most of their essential features. Particularly for V_d in the vicinity of V_c, it represents rather faithfully the position of the point P in Fig. 4 where the current on the high frequency side goes to zero; it is shown in Appendix B that this point lies at $\Delta\nu=\Delta\nu_c^*[(V_d/V_c)^2-1]^{\frac{1}{2}}$. As pointed out above, for V_d close to V_c, the initial phase δ_0 must be close to zero and for dee frequencies slightly less than $n\nu_R$, the protons will be very nearly always focused throughout their orbit in contrast to the case of dee frequencies slightly higher than $n\nu_R$, where the protons will be very nearly always defocused and lost. Therefore, independent of the details of transverse motion, the point P (Fig. 4) approaches, to a good approximation, the resonance frequency $n\nu_R$ as the dee voltage approaches the cut-off value V_c. It is principally this fact which allows us to derive the value of ν_R within about $\frac{1}{3}$ of the line width; in the absence of any theory the total width of the resonance curves would have to be considered as experimental error.

B. Perturbing Electric and Magnetic Fields

It is essential to investigate the effects of perturbing fields, particularly since a radial electric field will evidently cause a shift in the resonance frequency. Consider the case of a proton revolving in a circular orbit of radius r, and frequency ν_R in a magnetic field H which is in the z direction. The superposition of a small radial electric field E_r will appear to the proton as an additional magnetic field $\Delta H=-cE_r/2\pi r\nu_R$ and the fractional decrease in orbital frequency will be $\Delta\nu_R/\nu_R=\Delta H/H=-(E_r/E_0)\cdot(r_0/r)$, where $E_0=v_0H/c$ is the electric field necessary to cancel the Lorentz force due to the magnetic field H on the proton so that it would travel in a straight line with a velocity $v_0=r_0 2\pi\nu_R$. Actually, this is the electric field between the compensating electrodes (Fig. 1) and r_0 is the radius of injection. Taking $E_0=11{,}000$ volts/cm and $r_0/r=5$, one finds that a radial field of 0.01 volt/cm will cause a frequency error of one part in 2×10^5.

A similar expression for the frequency shift has been obtained by a perturbation calculation in which the radial and tangential components of a general perturbing electric field as seen by the proton were expressed as fourier series in the polar angle θ. From this calculation it is found that the only form of general field which will cause a frequency shift is one in which the radial component averaged over θ does not vanish. If this average is $\bar{E}_r$, then the fractional frequency shift is $\Delta\nu_R/\nu_R=-(\bar{E}_r/E_0)(r_0/r)$.

This perturbing field $\bar{E}_r$ may have several sources: (1) between the compensating electrodes there exists a strong dc field which fringes slightly into the dee cavity; (2) space charges may cause a small dc field; (3) the dees themselves produce rf fields which may partly contribute to $\bar{E}_r$; (4) the distortions of the field in the dees, due to the detector probe, may cause frequency shifts. It is believed that all of these sources of frequency error have been made negligible in the present experiment, as the following discussion will show.

The field from the compensating electrodes is shielded from the dee cavity by the injection plate (Fig. 1) and the alignment probe, which can be moved into a position where it acts as a shield. When this shield is moved down into the region of least shielding, a fan-shaped dc fringe field is admitted into the dee cavity, which causes a decrease in the resonance frequency of about one part in 6×10^3. This observed shift is in agreement with a calculation based on the measurement of the fan-shaped field of a two-dimensional model shaped like the cross section of Fig. 1. However, as the shield is moved upward into the effective shielding region, the frequency is observed to increase and then to remain stationary even as the shield is moved farther in. Thus, if the shield is beyond a certain position, the leakage field is made negligible, so that further shielding has no effect on the resonance frequency.

A calculation of the space-charge field of the protons themselves is difficult, owing to the uncertainty in the charge distribution. However, a crude calculation of this effect shows that there will be a radial electric field of the order of magnitude of $E_r\sim10^{-3}$ volt/cm, so that one expects a negligible frequency error. This expectation was confirmed by the observed experimental fact that a change in the entering proton current by a factor of 10 has no other effect than to change proportionally the magnitude of the detector probe currents without affecting their frequency dependence.

Likewise the charge produced by ionization of the gas in the dees has a negligible effect on the resonance frequency. At an air pressure of 10^{-6} mm Hg there is a probability of only 10^{-1} that a proton will produce one ion pair along a path consisting of 10^3 revolutions. The electrons will very rapidly leave the dee cavity, while the positive ions may have a lifetime at most about $\frac{1}{10}$ that of an orbital proton. Again, it is experimentally observed that a change of the gas pressure in the dee chamber by a factor of 10 has no effect on the frequency dependence of the probe current, which proves that space charges due to ionization are likewise negligible.

The cyclotron dees produce a perturbing electric field with primarily a θ-component which decelerates the protons. Because of the geometrical symmetry of the dees, the r-component averages to zero in one cycle and hence produces no frequency shift. However, any geometrical asymmetries of the dee configuration will cause a frequency shift.

The only essential asymmetry in the present arrangement is the detector probe (Fig. 1), which has been placed along a radius at $\theta=25°$ for structural reasons. Radio-frequency field lines terminate on this probe and the radial field component does not average to zero around a circle as it would do if the probe were at $\theta=0$. An upper limit to the frequency error, caused by the detector probe, has been estimated in the following manner: A two-dimensional electrostatic problem has been solved[14] in which the dees are represented by an

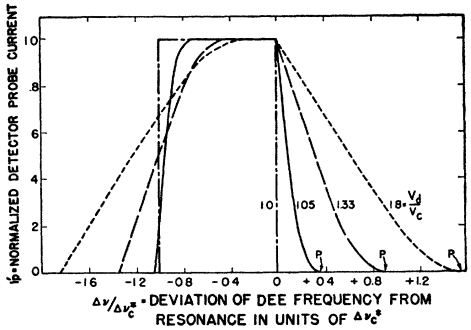

FIG. 4. Theoretical cyclotron resonance shapes, i.e., the detector probe current as a function of the dee frequency ν expressed in terms of $\Delta\nu/\Delta\nu_c^*$, where $\Delta\nu=\nu-n\nu_R$ and $\Delta\nu_c^*$ is the half width for a dee voltage $V_d=V_c$ given by Eq. (6). The curves plotted are from Eqs. (13A), (14A), and (15A) of Appendix B with the current normalized to unity at maximum amplitude.

[14] I am indebted to Mr. K. Trigger for having carried out this calculation.

infinite split cylinder and the probe by an infinite wire at a radius $r=0.4r_0$. With the top semi-cylinder at a potential of V_d volts and the wire and lower semi-cylinder at zero volts, the radial component of the field $E_r'=V_d f(\theta)$ along a circle of radius $r=0.5r_0$ has been calculated. This is an upper limit calculation because the shielding effect of the top and bottom of the dees is neglected. For resonance at the nth multiple the dee voltage is $V_d\cos(2\pi n\nu_R t)$, and the perturbing electric field will be

$$\bar{E}_r=\int_0^{2\pi} E_r'\cos n\theta d\theta.$$

Taking $V_d=200$ volts, one finds for $n=7$, $\Delta\nu_R/\nu_R=+1/4500$; for $n=9$, $\Delta\nu_R/\nu_R=+1/600{,}000$; for $n>11$, $\Delta\nu_R/\nu_R$ is extremely small.

These values are in essential agreement with the experimental results; the resonance frequency is observed to be the same for the 9th and 11th multiples, but at the 7th multiple it is increased by about one part in 1.5×10^4. Thus we conclude that the detector probe effect is negligible at the 9th and higher multiples. This fact was verified further by an experiment in which a dummy detector probe identical to the actual detector probe was installed in the dees at an angle $\theta=-25°$ and at a slightly smaller radius than the actual detector. This removed the geometrical asymmetry but still allowed the spiraling protons to strike the actual detector first. It was observed that at the 9th multiple the presence or absence of the dummy probe did not change the resonance frequency under otherwise identical operating conditions, whereas at the 7th multiple, the addition of the dummy probe caused the resonance frequency to decrease by about one part in 1.5×10^4, and thus to agree with the 9th and 11th multiples. Hence, by the use of a dummy probe the perturbing effect of the detector probe can be canceled for all dee frequencies. Another effect of the detector probe is due to the fact that, in collecting protons, it reaches a voltage slightly above that of the grounded dee into which it protrudes and thus causes a static electric field. With this voltage only of the order of 10^{-3} volt, the corresponding frequency shift is evidently negligible.

In addition to the possibility of causing frequency shifts, electric fields can cause a drift of the proton orbit. A uniform field in the plane of the orbit of the order of 0.1 volt/cm may cause, after 10^3 turns, a displacement of $0.05r_0$, which would be interpreted as a slight broadening of the resonance bandwidth. However, there are no conceivable sources of uniform fields of this magnitude inside the dees.

Magnetic field perturbations may be of several types: (1) random or consistent space variations in the field H; (2) radio-frequency fields produced both by displacement currents and by real currents flowing in the dees; (3) the field produced by the proton current. This latter field is utterly negligible, being of the order of 10^{-9} gauss for the proton currents used in this experiment.

A space variation of the field by an amount $\Delta H/H$ within the area of the proton orbit will evidently set a lower limit to the resonance bandwidth by the amount $\Delta\nu_R/\nu_R\sim\Delta H/H$. If this variation is random, the proton orbit will not be particularly affected, but a consistent variation due to a tilt of the pole pieces will cause a drift of the orbit; this drift may be estimated as follows. A proton revolving in a circular orbit of radius r and frequency ν_R in a field H in the z direction may be considered as a system with a magnetic moment $\mu_z=e2\pi\nu_R r^2/2c$. If the field H increases slightly in the x direction at a constant rate dH/dx, this will produce on the system a force $F_x=\mu_z dH/dx$ and result in a drift with uniform velocity v such that the Lorentz force F_x' on the drifting system will be equal and opposite to F_x. With $\mathbf{F}'=(\mathbf{v}\times\mathbf{H})e/c$ one obtains thus $F_x'=-Hev_y/c=-\mu_z dH/dx$, and for the drift velocity $v_y=(er^2/2Mc)(dH/dx)$. In N revolutions the center of the orbit will therefore drift a distance $y=rN\Delta H/H$, where $\Delta H/H=(r/H)(dH/dx)$.

As described in Sec. III, the magnetic field in the interior of the dees has been made quite uniform, the maximum variation over the distance r_0 being $\Delta H/H=\pm1/25{,}000$. Because of the transit time effect, most of the orbit revolutions occur at a radius which is considerably smaller than the initial radius r_0 and at a consequently smaller value of $\Delta H/H$. It is estimated that under typical experimental conditions the magnetic field inhomogeneities limit the resonance bandwidth to about one part in 7×10^4; actually, other factors limit the observed bandwidths to several times this value.

From Fig. 7 it can be seen that the field non-uniformity consists chiefly of a consistent tilt. Taking $r_0/2$ as an average value of r, for which $\Delta H/H\simeq1/50{,}000$, one calculates a drift distance in 10^3 revolutions of $y=10^{-2}r_0$. Thus, this drift will have a negligible effect on the mechanics of the orbital motion as previously discussed.

If the dee voltage is $V_d\cos(2\pi n\nu_R t)$, then the magnetic field H_d produced by the displacement current is of the order of magnitude $H_d\simeq2\pi n\nu_R V_d/c$ and has components which are parallel to the field H. At the higher multiples the rapid oscillations of H_d will result in an effective perturbing field $\bar{H}_d$ which is decreased by approximately a factor $1/n$. Thus, a reasonable estimate of the frequency error due to displacement currents is $\Delta\nu_R/\nu_R=\bar{H}_d/H=eV_d/Mc^2=1/(3\times10^6)$ for a typical dee voltage.

The real rf currents flowing in the dees and lead wires may produce a field having components parallel to the field H. With symmetrical dee geometry and lead wires, this field, from the viewpoint of the proton, averages to zero in one revolution. Thus, the symmetry of the dee geometry in the present experiment removes the possibility of frequency errors due to rf dee currents. However, the dee leads are somewhat asymmetric, but a calculation has shown that this causes a maximum frequency error of one part in 3×10^5.

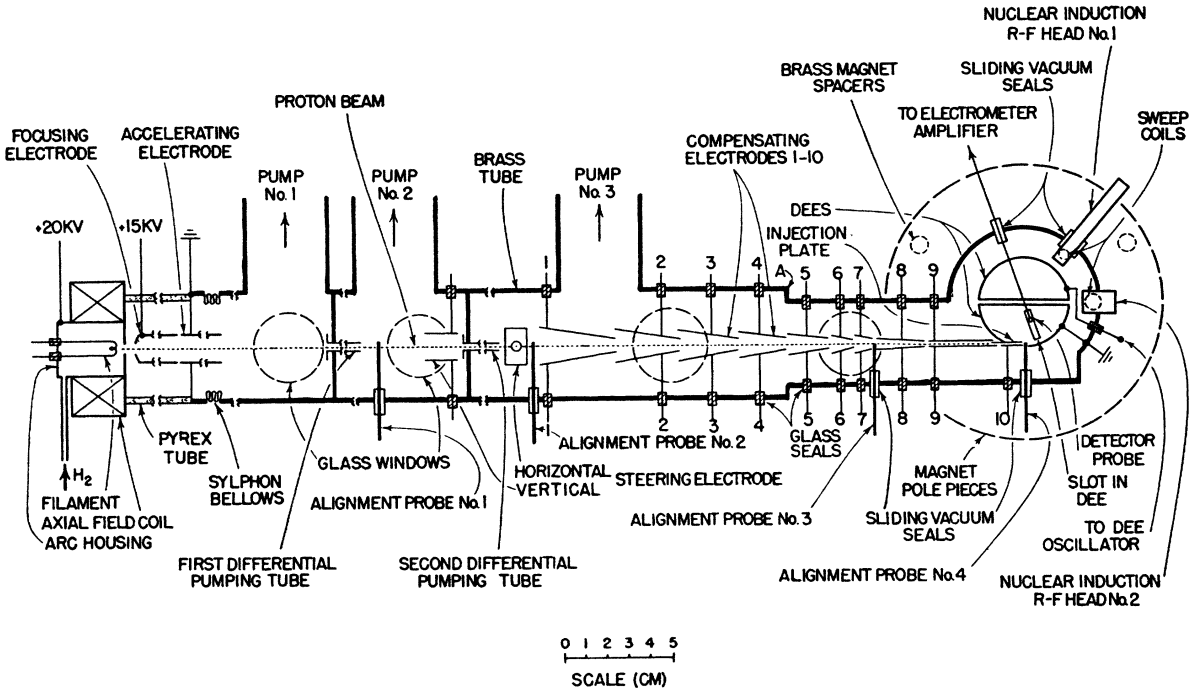

FIG. 5. Detailed drawing of apparatus.

III. DESCRIPTION OF APPARATUS

A detailed scale drawing of our apparatus is given in Fig. 5, and an electrical block diagram in Fig. 6. The operation in reference to this drawing is, very briefly, this: protons from the arc source are accelerated to 20 kv; they pass through the differential pumping stages and enter into the field of the magnet, where the Lorentz force on them is cancelled by the electric field of the compensating electrodes; finally the protons enter the dees where they are decelerated by the dee voltage until they strike the detector probe near the center.

The arc source is of conventional design, utilizing an axial magnetic field of several hundred gauss to enhance the ionization of hydrogen gas, which enters through a palladium leak, by collision with electrons from a hot tantalum filament. With the filament at 50 v below the arc housing, the arc current is about $\frac{1}{2}$ amp. Protons are pulled through a 1 mm hole in the arc housing by a cylindrical focusing electrode at an adjustable potential of about 5 kv below the arc housing. Coaxial with this electrode is a second accelerating electrode at a fixed potential of 20 kv below the arc housing. These electrodes constitute a proton gun which produces a proton beam of 1 μamp. about 3 mm in diameter. The proton gun is aligned with respect to the rest of the apparatus by means of a sylphon bellows.

The gas pressure in the arc is normally about 10^{-2} mm Hg and about 10^{-4} mm Hg in the region of the accelerating electrode, which is evacuated by pump No. 1. In order to maintain considerably lower pressures in the dee cavity, it has been necessary to employ differential pumping; the collimated proton beam from the gun passes through the first differential pumping tube into an intermediate region evacuated by pump No. 2, whereby the gas pressure is reduced to about 3×10^{-6} mm Hg without appreciable reduction in the beam current; the process is repeated with a second differential pumping tube, allowing an ultimate gas pressure of about 5×10^{-7} mm Hg in the region containing the dees, which is evacuated by pump No. 3. The pressure in this region is limited by outgassing and small leaks, and is independent of the pressure in the arc source.

The differential pumping tubes have a diameter of 3 mm and are 8 cm long. The pumps are 4-inch metal oil diffusion pumps equipped with cold vapor traps containing solid CO_2 or liquid nitrogen. All pressures have been measured with D.P.I. Type VG-1A ionization gauges. Because of the high speed of the pumps, little difficulty has been experienced in maintaining the vacuum. Except for a Pyrex glass pipe in the proton gun, the vacuum system is constructed of brass or copper, the joints being made with rubber gaskets. Electrical leads are brought through either Kovar or platinized glass seals.

In addition to the detector probe in the dees, there are four probes which, together with horizontal and vertical steering electrodes, are used to properly align the proton beam. All these probes operate through sliding vacuum seals of the Wilson type. Both the alignment probes and the ends of the differential pumping tubes are coated with a fluorescent substance and are visible through glass windows; this facilitates alignment and makes it possible to observe the shape of the beam.

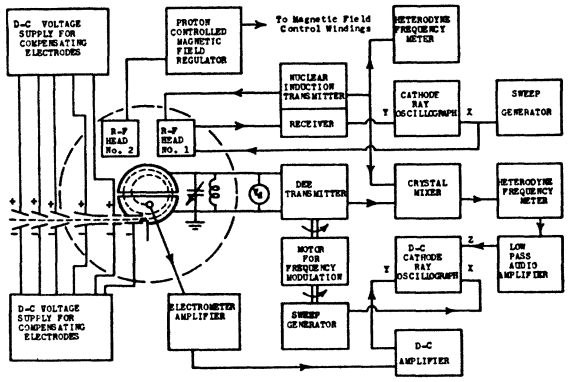

FIG. 6. Electrical block diagram of apparatus.

The compensating electrodes have been designed to provide, along a straight-line path, an electric force on the protons equal and opposite to the Lorentz force due to their motion in the magnetic field; this compensation is made to extend out to a distance about equal to the pole-piece diameter, and it requires ten pairs of tilted electrode plates for this purpose. The protons enter along a line in the median plane of the magnet gap, and the fringe field is essentially perpendicular to the proton path. By measuring the magnetic field with a flip coil, it has been possible to graphically determine the arrangement and shape of the ten pairs of tilted plates which will give an electric field perpendicular to the magnetic field and vary in magnitude approximately in the same manner along this line. The voltage for each pair of electrodes is balanced to ground, so that the potential along the proton path remains at zero. Each electrode is supplied by a separate voltage divider across a common center-grounded dc supply, whose overall voltage may be varied by a single control. This provides single-control adjustment of the compensating field for any value of the magnet current and also allows for local adjustments. By the help of the alignment probes, it is possible to adjust the relative electrode voltages so that the proton path is essentially a straight line, with a proton current of about 10^{-9} amp at alignment probe No. 4.

The protons enter the lower (grounded) dee tangentially to the injection plate which is attached to it. This plate is 0.25 mm thick and extends over the width of the dee. Together with the alignment probe No. 4, which has also the width of the dee, this plate very effectively shields the interior of the dee cavity from the field of compensating electrode No. 10. The dees are made of 0.16 cm thick copper and have an inside radius of 4.25 cm and an inside width of 1.65 cm. They are centered both radially and axially in the magnet gap. The grounded dee is slotted on one face to admit the detector probe, which is variable in position along a radius at an angle of 65° with respect to the dee gap. This probe is a small copper strip 1 mm wide and 0.1 mm thick, extending over the width of the dee and parallel to the magnetic field. The upper dee has a hole in the side wall to allow the nuclear induction head No. 1 to be moved from its normal position (as shown in Fig. 5) at a radius of 6.7 cm into the center of the dees. This motion is accomplished through a sliding vacuum seal and provides a simple means of measuring H/H', the ratio of the magnetic fields of nuclear resonance and orbital motion in Eq. (2). The dees, the various probes and compensating electrodes, as well as the nuclear induction head No. 1, are mounted in a vacuum chamber, called the cyclotron head, which may be dismounted from the pump tube at point A (Fig. 5) and removed from the magnet gap. We have carefully avoided the use of ferromagnetic materials in the cyclotron head.

The dees are resonated by a parallel coil and variable condenser (Fig. 6) and are excited by a modified Signal Corps Type ARQ-8 transmitter, which consists of a tunable oscillator and two tunable stages of amplification; it provides about 50 watts of rf power in the frequency range 20 to 90 Mc/sec, which is sufficient for operation of the cyclotron at any odd multiple of ν_R from the third to the eleventh, inclusive. For operation at $\nu_R \cong 8$ Mc/sec we have used a modified Signal Corps Type BC 459 A transmitter. To facilitate the observation of resonance, described below, the frequency is varied by a small amount in the neighborhood of $n\nu_R$ by means of a motor driven butterfly condenser at a rate of $\frac{1}{4}$ cycle/sec. The detector probe currents are of the order of magnitude of 10^{-12} amp for the higher multiple frequencies and are amplified by a balanced electrometer circuit,[15] utilizing a pair of Victoreen UX41-A tetrodes. The input resistance of the amplifier is 10^9 ohms; due to the capacitance in the coaxial lead from the probe to the tetrodes, the time constant is limited to about 10^{-2} sec. The time required to sweep through resonance is about one second, which is sufficiently larger than the detector time constant to prevent any appreciable distortion of the resonance shapes.

The nuclear induction apparatus for observing the nuclear resonance of protons consists of a transmitter-receiver unit and the r—f head No. 1 (Fig. 5) and is of the usual design.[8,16,17] The rf head is designed to fit inside a brass tube 1.25 cm in diameter so that it can be moved into the dee cavity. The proton sample, a 0.02-molar solution of $MnSO_4$ in pure H_2O, is cylindrical in shape with a volume of 0.1 cc. The sweep coils are 2.5 cm in diameter and are mounted coaxial with the sample on the outside walls of the cyclotron head.

We have used a single-yoke, air-cooled electromagnet with circular plane pole pieces 26.4 cm in diameter, spaced 4.80 cm apart. There are two coils, requiring 7.2 amp at 60 volts to produce a field of 5300 gauss; within about 0.3 percent, this is the field value at which we have operated throughout the experiments. The magnet

[15] J. A. Victoreen, Proc. Inst. Radio Engrs. **37**, 432 (1949).
[16] W. G. Proctor, Phys. Rev. **79**, 35 (1950).
[17] M. E. Packard, Rev. Sci. Instr. **19**, 435 (1948).

power is supplied by a 125-volt dc generator which is connected to the coils through a 9 ohm resistor. To reduce current fluctuations due to fluctuations in the generator voltage, a 60-volt bank of automobile storage batteries is connected directly across the coils; these "floating" batteries provide a regulation factor of about 100 by virtue of their low internal resistance. The value of the field can be finely controlled by means of a 2000-ohm variable resistor in parallel with the magnet coils. To achieve a still higher constancy of the field value, we have employed a proton-controlled magnetic field regulator as described by Packard.[17] This apparatus obtains its information from the nuclear induction r—f head No. 2 (Fig. 5) and controls a current of about 0.1 amp in a pair of auxiliary coils around the magnet pole pieces. By this means the field can be maintained constant to within 1/200,000 for times of the order of $\frac{1}{2}$ hour. This stabilization has been used in the precise mapping of the magnetic field necessary to obtain extreme homogeneity.

With the cyclotron head removed from the magnet gap, field inhomogeneities have been measured by noting the change in the proton resonance frequency upon the displacement of a movable nuclear induction head from the center of the pole pieces to the point under observation; during this procedure the field is held to a constant value by the regulator described above. By this method it was possible to detect relative field variations down to 1/200,000.

When the magnet coils are energized, there occurs normally a considerable bending of the magnet yoke, which tends to make the pole faces non-parallel. This effect has been prevented to a large extent by the use of two brass spacers (Fig. 5) which are inserted when the field is zero. Further field corrections have been made by ferromagnetic "shims," which were held to the pole faces by thin brass caps; circular rings of 0.01 cm steel shim stock have been used near the edges of the pole faces; nickel, electroplated on brass shim stock to a thickness of about 2×10^{-4} cm, has been used in a trial-and-error process to make the field still more homogeneous in a circle of about 3.9 cm radius, which is the maximum radius of the proton orbit.

In order to obtain consistent reproduction of the magnetic field configuration in this region, it has been found necessary to operate the magnet within a temperature range between 38° and 43°C, and to employ a current cycling procedure whenever the coils are energized; it consists in increasing the current to about 30 percent above its normal value, then decreasing it to normal, repeating the procedure for about five times.

By taking these precautions it has been possible to achieve and maintain a homogeneous field in the region of the dees, which does not vary from the center value by more than 1/25,000. Figure 7 is a plot of the field configuration in terms of the fractional variation from the center value; it is an average of seven independent measurements. The deviation of any one measurement

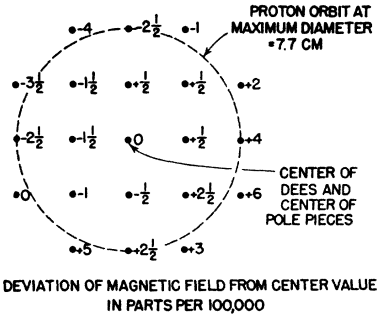

FIG. 7. Plot of the variation of the magnetic field within the region of the proton orbits.

from the average is about 1/200,000. The measurements were taken on several different days, spaced as widely apart as a month in one case, during which time the cyclotron head was installed in the magnet gap and most of the final data were obtained. The field in the local region of nuclear induction head No. 1 is also very homogeneous.

Although the field within the proton orbit is reproducibly homogeneous, it has been found that the value of the field, at the position of nuclear induction head No. 1 relative to that at the center, may vary from day to day by as much as 1/20,000, while only a very small variation occurs over a period of a few hours. For this reason we have constructed the nuclear induction head No. 1 to be movable between the normal monitoring position and the dee center, so that the field ratio H/H' of Eq. (2) can be measured directly to high accuracy. In the present experiment a typical value is $H/H'=(1-1/30{,}000)$.

As is shown in the block diagram of Fig. 6, the end result of the overall operation of the apparatus is the oscillographic presentation of the two resonance phenomena involved. The nuclear induction signals are displayed in the usual manner on an oscillograph by superimposing upon the constant field H', by means of the sweep coils (Fig. 5), a 60-cps sinusoidal field of about two gauss and applying a horizontal sinusoidal sweep of the same frequency and adjustable phase; the rf leakage into the receiver coil has been adjusted so that a pure absorption mode is observed.

The cyclotron resonances are observed by a small frequency modulation of the dee transmitter at a rate of $\frac{1}{4}$ cycle/sec and a sawtooth horizontal sweep of the same rate applied to a DuMont Type 304-H dc oscillograph with a long-persistence screen. The detector probe currents, amplified by the electrometer circuit and a subsequent single-stage dc amplifier, are applied to the vertical plates of this oscillograph. With the horizontal sweep phased to begin (and end) when the dee frequency is a maximum, a trace such as that of Fig. 8 is obtained; it is apparent that resonance is swept through twice, first with the dee frequency decreasing and then with it increasing.

A record of the dee frequency is made on the trace by

modulation of the intensity of the cathode-ray tube with the audio beat, amplified by a low-pass amplifier, from a heterodyne frequency meter tuned either to: (1) a fixed frequency within the range over which the dee transmitter is modulated, or to (2) a frequency which is the difference between the dee frequency and a harmonic of the nuclear induction frequency. This intensity modulation provides two frequency markers which appear as the bright spots A, A′ on the trace of Fig. 8.

In case (1) above, the dee frequency ν has been measured with a Signal Corps Type BC-221 Q heterodyne frequency meter while at the same time ν_N has been measured with a very similar instrument—a Navy Type LM-18 meter. By calibrating both meters with the crystal from only one of them, it is possible to make a relative measurement of ν and ν_N to an accuracy within about 1/50,000, this limitation being set by the reading of the dial.

Case (2) above has been used at the 9th multiple cyclotron frequency to obtain greater accuracy than case (1) affords. As shown in Fig. 6, it requires a mixer tuned on the input to $\nu \cong 9\nu_R$ and to ν_N, and on the output to $\nu'' = \nu - 3\nu_N \cong 9\nu_R - 3\nu_N = \nu'$. The frequency ratio $\mu = \nu_N/\nu_R$ in Eq. (2) can then be written in the form $\mu = 9\nu_N/(\nu' + 3\nu_N)$, and one obtains for the relative error of measurement $\delta\mu/\mu = \pm[\nu'/(\nu' + 3\nu_N)][(\delta\nu'/\nu')^2 + (\delta\nu_N/\nu_N)^2]^{\frac{1}{2}}$. Thus, the accuracy of measurement of the frequencies is made less critical by the factor $\nu'/(\nu' + 3\nu_N) \cong 1/15$. We have used the Signal Corps BC-221Q meter to measure ν'', while at the same time ν_N has been measured with the Navy LM-18 meter. In this case we have calibrated each meter with its own crystal, observing that the crystals do not differ in frequency by more than 1/25,000. This allows a measurement of ν_N/ν_R with an error of only about $\pm 1/250{,}000$.

As is shown in Fig. 8, the frequency markers A, A′ occur on the trace slightly displaced from their true position because of a time delay in the amplifiers. In terms of frequency this displacement corresponds to a shift of about 1/50,000 and can easily be corrected for by moving the markers forward on the photograph until they are at mirror symmetrical positions B, B' on the two halves of the trace. Another advantage of sweeping through resonance both with increasing and decreasing dee frequency, is that it shows the absence of distortion of the two resonance curves because of the observed fact that they are symmetrical about the center of the trace.

FIG. 8. Photograph of a typical cyclotron resonance trace at the 9th multiple of ν_R. The vertical deflection is proportional to the detector probe current; in the horizontal direction, the dee frequency first increases and then decreases, thus sweeping twice through resonance. The two bright spots on the trace at A and A′ are the frequency markers, which are slightly displaced from their true positions B and B′ because of time delay in the amplifiers. The relative width at half maximum amplitude is about 1/9000 for this resonance curve.

IV. MEASUREMENTS AND INTERPRETATION

The following procedure has been used in the operation of the apparatus: First, with the magnet warmed up and the current turned on through the cycling procedure described in Sec. III, the field is adjusted to about 5300 gauss. The proton gun is put into operation and the voltages on the compensating electrodes are so adjusted that a proton beam enters the dees. Next, a measurement of H/H' of Eq. (2) is made by means of the sliding rf head No. 1; during this process the magnetic field is maintained constant either by the proton-controlled field regulator or by manual control of the magnet current, using the nuclear induction signals from rf head No. 2 as a field indicator. Rf head No. 1 is then returned to its normal position just outside the dees and the signals from it are used to observe the exact proton resonance frequency by adjusting the frequency until the traces are symmetrical about their center point. With the receiver adjusted for a pure absorption mode, this is a simple and sensitive method of ascertaining true resonance, as discussed by Jacobsohn and Wangsness.[18] The magnetic field is held to this resonance value either by the field regulator or by fine manual control of the magnet current; the latter method was necessary at the higher dee frequencies, where the regulator was unstable because of insufficient rf shielding from the dee transmitter. The dee transmitter frequency is then set to approximately $n\nu_R$ and varied slightly until resonance curves are observed on the dc oscillograph; the heterodyne frequency meter, which provides the frequency markers, is adjusted to give an intensity marker on the trace near the maximum of the resonance curve. Data are obtained by photographing a single trace (of 4 seconds duration) of the cyclotron resonance curve while at the same time another observer is holding the magnetic field to the value for exact nuclear resonance by means of visual observation of the nuclear induction signals and fine manual magnet current control. Immediately after the photographic exposure the marker frequency and the nuclear induction transmitter frequency are measured. The exposure and frequency measurement take about 10 seconds during which time frequency drifts are negligible and the magnetic field is held constant to within $\pm 1/100{,}000$. After photographing several resonance curves for various dee voltages and detector probe positions, H/H' is again measured and noted to be the same as before.

[18] B. A. Jacobsohn and R. K. Wangsness, Phys. Rev. **73**, 942 (1948).

We have observed cyclotron resonance at all odd multiples of ν_R from the 1st to the 11th. The most precise data were obtained at the 9th multiple; minor instrumental difficulties have so far prevented equally useful data at the 11th multiple. The detector probe position has been varied within the range $r/r_0=0.2$ to 0.8, and the dee voltage within the range $V_d=110$ to 350 volts peak. The observed detector probe currents are smaller at the higher multiple frequencies and decrease both as the detector probe is moved to smaller radii and as the dee voltage is decreased. The largest currents observed have been about 10^{-10} amp, and the smallest about 3×10^{-13} amp. The calculated Johnson noise current is about 4×10^{-14} amp; the observed background fluctuation is about twice as large as this value because of rf pickup, microphonics, amplifier drifts, etc. We have observed that a variation of the proton current entering the dees (e.g., by varying the arc filament heating) by a factor of 20 has no effect other than to vary the amplitude of the resonance signals; particularly, there are neither current dependent changes in the signal shape nor frequency shifts.

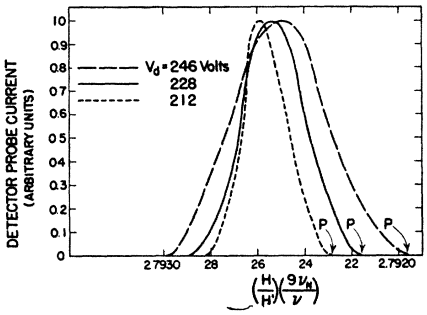

FIG. 9. Observed cyclotron resonance curves (normalized to unit amplitude) at the 9th multiple of ν_R for various dee voltages V_d. In each case the detector probe was at a position $r=0.4r_0$, and the cut-off voltage V_c was observed to be 206 volts. The dee frequency ν is given in terms of $(H/H')(9\nu_N/\nu)$. The points P correspond to the disappearance of the probe current on the high-frequency side.

The gas pressure in the dee chamber, as measured in the manifold to the pump, has been about 10^{-6} mm Hg during most of the measurements. At the 7th and 9th multiples we have varied the pressure in this region from about 5×10^{-7} mm Hg to about 10^{-5} mm Hg. Under otherwise identical operating conditions this variation does not change the shape or resonance frequency of the cyclotron resonance signals. The only pressure effect is a decrease of the signal magnitude; at a pressure of about 2×10^{-5} mm Hg the signals have fallen to the noise level and are no longer observable. This is in rough agreement with an exponential dependence of the current I upon the pressure P (in mm Hg) of the form $I=I_0\exp(-2.6\times10^5P)$ which one obtains for a proton making 500 revolutions at an average radius of 2 cm and taking a total gas kinetic scattering cross section of 1.25×10^{-15} cm^2. In view of this agreement and the experimental fact that neither the resonance frequency nor the bandwidth are pressure dependent, we have not made a detailed analysis of scattering effects. Because of scattering in the plane of the dees, one would expect a pressure broadening of the resonance bandwidth. We have not observed this in the present experiment, evidently because the probability that a proton be scattered sufficiently in the transverse direction to be lost, is considerably greater than the probability that it be scattered sufficiently in the median plane to cause a resonance broadening.

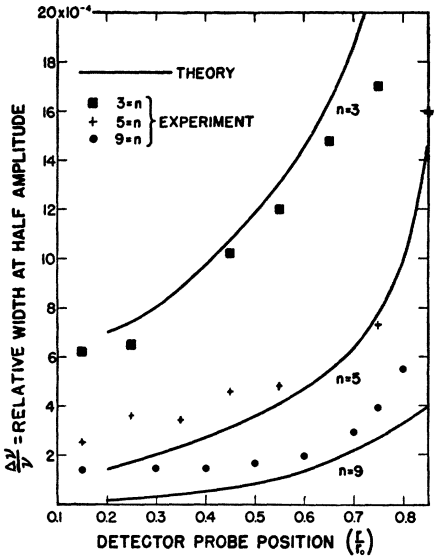

FIG. 10. Comparison of the theoretical and experimental relative widths at half maximum amplitude of cyclotron resonance curves for various detector probe positions. The data have been obtained at the 3rd, 5th, and 9th multiples of ν_R with a fixed dee voltage for each multiple. It was: $V_d/V_c=176/127$, $179/141$, and $247/223$, for the 3rd, 5th and 9th multiples respectively. Using these values of V_d/V_c, the theoretical half width has been obtained from the formulae in Appendix B.

The traces, like that of Fig. 8, are not drawn on the oscillograph in a linear frequency scale because frequency modulation is obtained by rotation of a butterfly condenser. However, the tuning curve of this condenser may be easily measured, and Fig. 9 shows several typical resonance curves for various dee voltages replotted on a linear frequency scale in terms of $(H/H')(n\nu_N/\nu)$. These curves have been normalized to unit amplitude; the actual signal amplitude at the highest dee voltage is about 10 times larger than that at the lowest.

As a first check on the theory of Sec. II we compare the relative width at half maximum amplitude of observed curves like those of Fig. 9, with the corresponding width of theoretical curves like those of Fig. 4. This comparison is given in Fig. 10 as a function of the detector probe position for a fixed dee voltage at the 3rd, 5th, and 9th multiples. The fairly good agreement at the 3rd multiple between the experimental points and the theoretical curve indicates that here the focusing action is sufficient to confine the protons to approximately the median plane of the dees, which was assumed

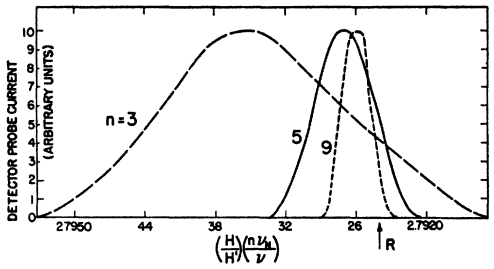

FIG. 11. Observed cyclotron resonance curves (normalized to unit amplitude) for operation at the 3rd, 5th, and 9th multiples of ν_R. The dee frequency ν is given in terms of $(H/H')(n\nu_N/\nu)$. In each case the detector probe was at $r=0.36r_0$ and the dee voltage V_d was about $1.05V_c$. The common point of the curves is approximately at R, where $n\nu_N/\nu=2.7924\cong\nu_N/\nu_R=\mu_p/\mu_n$.

in the theory. We attribute the poorer agreement at the 5th and 9th multiples, particularly at probe positions near the center, to the fact that the protons oscillate with appreciable amplitude about the median plane due to the weaker focusing action in this case. The assumption that they oscillate with increasingly greater amplitude as the radius decreases is supported by the fact that the observed bandwidth is about the same at the 9th multiple for all probe positions less than about $r=0.4r_0$.

The theoretical expectation (Sec. II) that phase focusing causes the resonance point to lie near the higher frequency side of the curves is verified in Fig. 11, which shows observed resonance curves at the 3rd, 5th, and 9th multiples replotted on a linear frequency scale in terms of $(H/H')(n\nu_N/\nu)$. In each case the dee voltage was about 5 percent greater than the cut-off value V_c. A dummy probe was used at the 3rd and 5th multiples to cancel frequency shifts due to the detector probe (Sec. II). The curves are evidently similar in shape, with a corresponding point at the approximate position R, where $(H/H')(n\nu_N/\nu)=2.7924$; interpreting this point as an indication of resonance, the same value may be taken to be the desired ratio μ_p/μ_n.

Although this method of deducing μ_p/μ_n from the data serves indeed as a valuable check, we have used

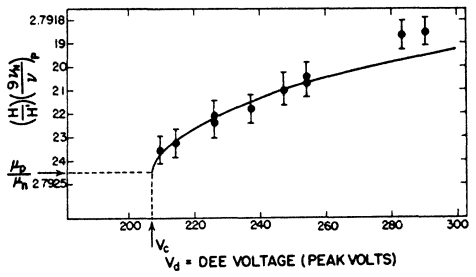

FIG. 12. The variation of observed values of $(H/H')(9\nu_N/\nu)_P$ with the dee voltage V_d for cyclotron operation at the 9th multiple of ν_R, and a detector probe position at $r=0.26r_0$. The solid curve is the expected approximate theoretical behavior and is a plot of Eq. (7) for $n=9$, where $V_c=207$ volts (observed value), $\Delta\nu'/9\nu_R=1/5600$ (observed total resonance bandwidth for $V_d=1.04V_c$), and $\mu_p/\mu_n=2.79245$ (graphically chosen to give a best fit to the experimental points).

the more quantitative procedure of observing the point P on the high frequency side of the resonance curves where the current goes to zero, as a function of the dee voltage at fixed values of n and the detector probe position. This point is indicated in Fig. 9 and corresponds to the point P in the theoretical curves of Fig. 4. The experimental points shown in Fig. 12 are observed values of $(H/H')(n\nu_N/\nu)_P$ corresponding to this point for various dee voltages near the 9th multiple of ν_R with the detector probe at $r=0.26r_0$. As shown in Sec. II, it is theoretically expected that this point approaches the true resonance value as the dee voltage V_d approaches the cut-off value V_c. However, as V_d approaches V_c, the signal amplitude decreases steadily so that a measurement of $(H/H')(n\nu_N/\nu)_P$ is difficult for V_d very near V_c. Therefore, we have extrapolated the data to V_c by using the expression

$$(H/H')(n\nu_N/\nu)_P = \mu_p/\mu_n[1-(\Delta\nu'/n\nu_R)((V_d/V_c)^2-1)^{\frac{1}{2}}], \quad (7)$$

which is obtained from Eq. (17A) (Appendix B) after replacing the theoretical bandwidth $\Delta\nu_c^*/n\nu_R$ by the actual observed bandwidth $\Delta\nu'/n\nu_R$. A plot of Eq. (7) is represented by the parabolic curve in Fig. 12. The value $\mu_p/\mu_n=2.79245$ has been obtained by extrapolation of the curve which best fits the experimental points, particularly for V_d in the vicinity of V_c; the agreement is fairly good considering the approximations made in the derivation of the curve. Furthermore, the above procedure applied to a set of data taken at a different probe position yields essentially the same value of μ_p/μ_n.

Another check has been obtained by applying this same procedure at the 3rd, 5th, and 7th multiples also, with the result in each case that the value of μ_p/μ_n obtained is in good agreement with that for the 9th multiple. This consistency, together with the excellent agreement of this value with the value of $(H/H')(n\nu_N/\nu)$ at point R of Fig. 11, provides assurance that our interpretation of the cyclotron resonance is essentially correct.

V. CALCULATION OF μ_p/μ_n

The value of μ_p/μ_n reported here is based upon a total of 135 individual cyclotron resonance observations, arranged in 17 groups. In each group of data, all the significant experimental parameters are held constant except the dee voltage. For each group $(H/H')(n\nu_N/\nu)_P$ has been plotted *versus* V_d and the parabolic curve of Eq. (7) has been fitted to the experimental points as in Fig. 12 in order to determine μ_p/μ_n. A summary of the data is given in Table I, where the best fitting value of μ_p/μ_n and the graphical fitting error have been determined by making several trials of fitting in each case. The data at the 3rd, 5th, and 7th multiples have been obtained with a dummy probe at $r=0.35r_0$ to prevent frequency shifts.

The average value of μ_p/μ_n from this table is 2.79242, and the mean deviation from this average value is about

1/74,000. This variation is not due to any internal inconsistency in the data, but is the result of statistical errors of measurement, which are estimated to be as follows:

(1) $\pm 1/100{,}000$ due to errors in setting the nuclear induction signal to exact resonance because of inexact adjustment of the receiver to a pure absorption mode.

(2) $\pm 1/100{,}000$ due to drift of the H field during observation of resonance.

(3) $\pm 1/75{,}000$ due to errors in the measurement of H/H'.

(4) $\pm 1/50{,}000$ due to errors in frequency measurements at the 3rd, 5th, and 7th multiples. This error is reduced by a factor 5 at the 9th multiple, as discussed in Sec. III.

(5) $\pm 1/100{,}000$ due to errors in correction of the frequency marker position (see Fig. 8) and correction of the non-linearity of the frequency scale of the traces.

(6) $\pm 1/50{,}000$ due to the average magnetic field inhomogeneity over a proton orbit; this is less than the inhomogeneity across the dee diameter because the transit time effect causes most of the proton revolutions to occur at smaller radii, where the field is more homogeneous.

Since these errors are statistically independent, we take the root of the sum of their squares as an indication of the over-all statistical error of any one measurement; this is $\pm 1/29{,}000$ for the 3rd, 5th, and 7th multiples and $\pm 1/34{,}000$ for the 9th multiple. Reducing these by $1/6^{\frac{1}{2}}$, where 6 is the average number of measurements used in a graphical calculation of μ_p/μ_n, we get about $\pm 1/80{,}000$, which agrees essentially with the statistics of Table I.

In order to obtain a good estimate of the absolute accuracy of our result, we have investigated all conceivable sources of systematic errors:

(1) Possible shifts in the cyclotron resonance frequency due to perturbing electric and magnetic fields have been discussed in detail in Sec. II, where it is shown that such errors are negligible, the total effect being to raise the observed value of μ_p/μ_n by about 1/500,000.

(2) The relativistic proton mass variation is $\Delta M/M = 1/100{,}000$ at an energy of 10 kv, which is approximately the average energy of the protons during their cyclotron orbit.

(3) Magnetic impurities in the movable nuclear induction head may cause an error of at most $+1/200{,}000$ in the measured value of H/H'.

(4) The paramagnetism of the manganese ions dissolved in the proton water sample increases the observed nuclear resonance frequency by a small amount. Using the calculations of Bloembergen and Dickinson[19] we find this to be about 1/400,000 for our 0.02 Molar sample.

(5) The magnetic field due to the electrons surrounding the protons in the water sample reduces the observed nuclear resonance frequency to some extent. In the absence of accurate knowledge of the size of this error we use the value $-1/37{,}000$, which has been calculated by Ramsey[20] for the case of an H_2 gas sample; preliminary measurements in this laboratory by M. Packard and E. Hahn have indicated that the resonance frequency of protons in H_2 gas and in H_2O in the same magnetic field do not differ significantly for our purpose here.

To obtain an estimate of the overall systematic error we take the algebraic sum of the above errors; this is 1/140,000 and tends to make the values of μ_p/μ_n in Table I too low by this amount.

There is still another systematic error, arising from the use of our approximate analysis of the cyclotron resonance curve in locating the point of true resonance on this curve. This error is in the nature of an uncertainty which can only be estimated. In view of the generally fair agreement of the observed data with the approximate theory presented here, we believe that our analysis has not systematically misinterpreted the location of true cyclotron resonance by more than about $\frac{1}{3}$ of the total bandwidth of the resonance curves observed at the higher multiple frequencies; this corresponds to an error of about $\pm 1/14{,}000$. Considering that, compared to this error, all other errors both systematic and statistical are negligible, and using the average of the values in Table I, we can state our final result to be

$$\mu_p = (2.7924 \pm 0.0002)\mu_n. \quad (8)$$

This value is in essential agreement with the latest result reported by Hipple, Thomas, and Sommer,[11] which is

$$\mu_p = (2.79268 \pm 0.00006)\mu_n. \quad (9)$$

With the limits of error of the results of Eqs. (8) and (9) just touching each other, they can still be considered

TABLE I. Summary of data.

Cyclotron frequency multiple n	Detector probe position r/r_0	Number of measurements	Best fit value of μ_p/μ_n	Graphical fitting error in μ_p/μ_n
9	0.50	5	2.79239	±0.00002
9	0.40	7	2.79244	±0.00004
9	0.31	6	2.79238	±0.00006
9	0.26	6	2.79235	±0.00007
9	0.21	3	2.79243	±0.00003
9	0.40	8	2.79245	±0.00004
9	0.31	5	2.79245	±0.00003
9	0.26	11	2.79245	±0.00002
9	0.21	6	2.79245	±0.00003
9	0.40	6	2.79242	±0.00003
9	0.31	5	2.79243	±0.00003
9	0.26	7	2.79243	±0.00002
9	0.21	7	2.79239	±0.00002
7	0.36	22	2.79250	±0.00005
7	0.36	12	2.79250	±0.00005
5	0.36	10	2.79242	±0.00002
3	0.36	9	2.79230	±0.00025

[19] N. Bloembergen and W. C. Dickinson, Phys. Rev. 79, 179 (1950).

[20] N. F. Ramsey, Phys. Rev. 77, 567 (1950).

as a gratifying mutual confirmation. A more severe test will be obtained as soon as the accuracy of our method is somewhat increased. This should be possible by modifications of the present apparatus, now in progress in this laboratory; it is anticipated that appreciably smaller cyclotron resonance bandwidths than reported here can be obtained by changing the dee proportions and extending the operation to still higher multiples of ν_R, as well as by the use of baffle plates in the dees to remove those circulating protons which do not move closely in the median plane and are a source of resonance broadening. This latter scheme requires a new arc-source of protons with a higher current output, which is now under construction. It is also expected that this modified apparatus will be used in the determination of mass ratios of the light ions.

We shall not enter here into a discussion of the relation of our result to the faraday, the mass ratio of proton to electron, and other fundamental constants. These relations have been discussed by DuMond[21] and by Hipple, Sommer, and Thomas.[11]

In conclusion, the author wishes to express his sincere appreciation to Professor F. Bloch for suggesting this experiment and the method of the decelerating cyclotron operated at multiple frequencies, as well as for much help and encouragement throughout the course of the work. It is a pleasure to acknowledge valuable discussions with Professor H. H. Staub on the design of the apparatus, and his very helpful advice during its construction. Thanks are also due to Dr. M. E. Packard for numerous suggestions and to Mr. Kenneth Trigger, Mr. Burton Stuart, Mr. Edward Wright, and Elizabeth Jeffries for their assistance in various phases of the work.

Appendix A

Taking the potential of the electric field of Fig. 2 to be $\Phi(x, y)$ with the boundary conditions $\Phi(+x, \pm b/2)=v_d$ and $\Phi(-x, \pm b/2)=0$, it can be shown that Φ is given by

$$\Phi(x, y)=v_d-\frac{v_d}{\pi}\arctan\left[\frac{\cos(\pi y/b)}{\sinh(\pi x/b)}\right], \tag{1A}$$

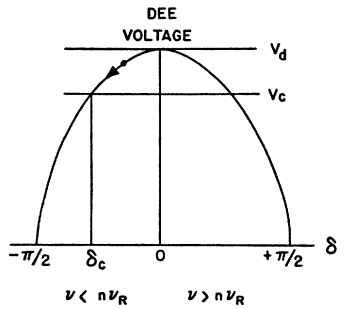

FIG. 13. Diagram of the variation of the dee voltage and its effective phase δ, experienced by a revolving proton in its consecutive passages through the dee gaps. For the case of a dee frequency below resonance, a representative point is indicated with the arrow showing the direction of the variation; for frequencies above resonance, the variation has the opposite direction.

[21] J. W. M. DuMond, Phys. Rev. 77, 411 (1950).

from which the components of the electric field E are seen to satisfy the relation

$$-E_x+iE_y=v_d/b\cosh(\pi z/b) \tag{2A}$$

where $z=x+iy$. Thus, near the median plane $y=0$, the field E_x drops in a distance $x=b$ to about $\frac{1}{10}$ of its value at the origin.

By taking $v_d=V_d\cos(2\pi\nu t+\delta)$, where δ is the phase angle of the voltage when the proton is at $x=0$, the energy change ΔE and the transverse momentum change ΔP_y of the proton in transit at a constant value of y from $x=-\infty$ to $x=+\infty$ at a velocity $dx/dt=v$ are given by the expression:

$$-\Delta E+iv\Delta P_y=e\int_{-\infty}^{+\infty}(-E_x+iE_y)dx$$
$$=\frac{eV_d}{b}\int_{-\infty}^{+\infty}\frac{\cos[(2\pi\nu x/v)+\delta]}{\cosh(\pi z/b)}dx. \tag{3A}$$

Evaluation[22] of this integral yields:

$$\Delta E=-eV_d\frac{\cosh(2\pi y\nu/v)}{\cosh(\pi b\nu/v)}\cos\delta, \tag{4A}$$

$$\Delta P_y=\frac{eV_d}{v}\frac{\sinh(2\pi y\nu/v)}{\cosh(\pi b\nu/v)}\sin\delta. \tag{5A}$$

Applying these equations to the actual case of a proton revolving in a circular orbit of radius $r=n v/2\pi\nu$ in dees of width b and radius R, and considering that the changes of r and y per revolution are small, so that differences can be replaced by differential quotients, we have

$$\frac{V_0}{r_0^2}\frac{dr}{dN}=-\frac{V_d}{r}\frac{\cosh(ny/r)}{\cosh(nb/2r)}\cos\delta, \tag{6A}$$

$$\frac{M\pi\nu^2}{n^2}\frac{d^2y}{dN^2}=\frac{eV_d}{r}\frac{\sinh(ny/r)}{\cosh(nb/2r)}\sin\delta, \tag{7A}$$

where N is the number of revolutions and eV_0 is the proton energy at a radius r_0. Because of the approximations made, these equations are approximately valid for $b\ll r<(R-b)$.

Taking $\sin\delta=\sin[\delta_0+(2\pi N\Delta\nu/\nu_R)]$ where $\Delta\nu=\nu-n\nu_R$ and δ_0 is the initial phase at $N=0$, we may integrate Eq. (6A) for $y=0$:

$$\sin[\delta_0+(2\pi N\Delta\nu/\nu_R)]-\sin\delta_0$$
$$=-\frac{2\pi\Delta\nu}{\nu_R}\frac{V_0}{r_0^2V_d}\int_{r_0}^{r}r\cosh(nb/2r)dr, \tag{8A}$$

where N is the number of revolutions in the proton orbit between r_0 and r. Taking the special case $\Delta\nu=0$, $\delta_0=0$, we find the expression

$$N(r)\Big|_{\substack{\delta_0=0\\ \Delta\nu=0}}\equiv N_0(r)=\frac{V_0}{r_0^2V_d}\int_r^{r_0}r\cosh(nb/2r)dr \tag{9A}$$

for the number of proton revolutions required to reach a radius r if the proton encounters the maximum dee voltage at each crossing of the gap. This integral can be evaluated from tables,[23] and is plotted in Fig. 3 as a function of r/r_0 with $V_d=200$ volts and n as a parameter; the constants have been chosen to correspond to the present experiment: $V_0=2\times10^4$ volts, $r_0=3.85$ cm, $b=1.65$ cm.

Appendix B

By neglecting focusing effects, an estimate of the resonance bandwidth for protons in the median plane may be obtained, as discussed in Sec. II. For a dee frequency ν slightly less than the resonance frequency $n\nu_R$ a proton will constantly slip in phase with respect to the dee voltage as it spirals in. This is represented in the phase diagram of Fig. 13 by a point moving toward negative δ. At the point where $\delta=-\pi/2$ the proton will have reached a minimum radius r and will be accelerated thereafter. A similar situation prevails at $\delta=+\pi/2$ for $\nu>n\nu_R$. Thus, if we take the initial phase $\delta_0=0$, then $\Delta\nu^*$, the maximum frequency deviation

[22] Bierens de Haan, *Nouvelles Tables D'Integrales Defines* (G. Stechert, New York, 1939), p. 387, No. 14.

[23] *Tables of Sine, Cosine and Exponential Integrals*, Volume I. (Works Progress Administration, New York, 1940).

from resonance for which a proton will just reach the detector probe at r, is obtained by taking $2\pi N\Delta\nu/\nu_R=\pi/2=\delta$ on the left side of Eq. (8A) and by using Eq. (9A), with the result

$$\Delta\nu^*/n\nu_R=1/2\pi nN_0. \tag{10A}$$

This expression may be interpreted as the half width of a symmetrical rectangular resonance curve to be expected under the idealized conditions of a well collimated proton beam and no focusing effects.

A refinement can be made by considering initial phase angles other than $\delta_0=0$ for fixed values of n and N_0. There are three different reasons for which a proton may not reach the detector probe: (1) it may not clear the injection plate; (2) the transition from deceleration to acceleration may take place at a radius larger than that at which the probe is located; (3) the transition from focusing to defocusing may take place before the probe is reached. All three reasons must be taken into account in the following considerations.

If V_c is the minimum dee voltage for injection, then a dee voltage of $V_d>V_c$ will inject protons with initial phases δ_0 for which

$$0\leq|\delta_0|\leq\arccos(V_c/V_d)=\delta_c.$$

Because of phase defocusing, we neglect, in the following discussion, all those with positive δ_0. For a given negative initial phase δ_0, all those protons will clear the injection plate (Fig. 1) for which the distance from the outer surface of the injection plate is less than $\Delta r=(r_0/2V_0)(V_d\cos\delta_0-V_c)$. We shall make the reasonable assumption that the incoming proton beam has a uniform distribution over a small thickness behind the injection plate. Therefore, the total injected beam current per unit initial phase angle will be proportional to the above expression for Δr and, in arbitrary units, can be written as $i(\delta_0)=V_d\cos\delta_0-V_c$. The detector probe current I_p can be obtained by integrating $i(\delta_0)$ over appropriate limits of δ_0. These limits are determined, below, by considering separately the cases of the dee frequency (a) slightly below and (b) slightly above the resonance frequency.

(a) In the case of dee frequencies slightly below resonance, there is a maximum absolute magnitude of the phase δ_0, which we designate by δ_0' and which is the particular value of the initial phase for which a proton will just reach the detector probe. Since the proton will reach its minimum radius when the phase δ has the value $-\pi/2$, one obtains from Eq. (8A) the following expression for determining δ_0':

$$\sin(-\pi/2)-\sin(\delta_0')=2\pi N_0\Delta\nu/\nu_R\equiv\gamma. \tag{11A}$$

For dee frequencies below resonance, γ is evidently negative. Let us consider first the case where $|\delta_0'|<|\delta_c|$; since protons with initial phases beyond δ_0' cannot reach the detector probe, I_p is obtained by integrating $i(\delta_0)$ between the limits $\delta_0=0$ and $\delta_0=-\delta_0'$. If, on the other hand, $|\delta_0'|>|\delta_c|$, then all the injected protons can reach the detector probe, so that one obtains in this case the maximum value of I_p; it is obtained by integrating $i(\delta_0)$ between the limits $\delta_0=0$ and $\delta_0=-\delta_c$. From Eq. (11A) and the definition of δ_c, it may be seen that the condition $|\delta_0'|<|\delta_c|$ corresponds to the condition $\gamma<-[1-(1-\alpha^2)^{\frac{1}{2}}]$ where $\alpha=V_c/V_d$. Furthermore, it is seen from Eq. (11A) that the maximum frequency deviation from resonance for which protons will just reach the detector probe is obtained for $\delta_0'=0$, which corresponds to $\gamma=-1$. Thus for $\gamma<-1$, I_p will be zero.

(b) In the case of dee frequencies slightly above resonance, there is a minimum absolute magnitude of the phase δ_0, which we designate by δ_0'' and which is the particular value of the initial phase for which a proton will just reach the detector probe at the instant at which the phase δ has reached the value zero; for later instances the phase δ will become positive, and the proton will be lost by defocusing. Similar to Eq. (11A), one obtains from Eq. (8A) the following expression for determining δ_0'':

$$\sin(0)-\sin(\delta_0'')=2\pi N_0\Delta\nu/\nu_R\equiv\gamma, \tag{12A}$$

where γ is now positive. Since the maximum value of $|\delta_0|$ is $|\delta_c|$, one obtains I_p by integrating $i(\delta_0)$ between the limits $\delta_0=\delta_0''$ and $\delta_0=\delta_c$. If $|\delta_0''|>|\delta_c|$, no injected protons may reach the detector probe before they are defocused, and I_p will be zero. The condition $|\delta_0''|>|\delta_c|$ corresponds to the condition $\gamma>(1-\alpha^2)^{\frac{1}{2}}$, as may be seen from Eq. (12A) and the definition of δ_c.

Performing the integrations indicated above, one thus obtains the following expressions for the detector probe current I_p:

for $-1<\gamma<-[1-(1-\alpha^2)^{\frac{1}{2}}]$,

$$I_p(\gamma)=V_d[1+\gamma-\alpha\arcsin(1+\gamma)]; \tag{13A}$$

for $-[1-(1-\alpha^2)^{\frac{1}{2}}]<\gamma<0$,

$$I_p=V_d[(1-\alpha^2)^{\frac{1}{2}}-\alpha\arcsin(1-\alpha^2)^{\frac{1}{2}}]; \tag{14A}$$

for $0<\gamma<(1-\alpha^2)^{\frac{1}{2}}$,

$$I_p(\gamma)=V_d[(1-\alpha^2)^{\frac{1}{2}}-\alpha\arcsin(1-\alpha^2)^{\frac{1}{2}}-\gamma+\alpha\arcsin\gamma]. \tag{15A}$$

These results are shown graphically in Fig. 4, in which the normalized detector probe current I_p' has been plotted *versus* γ/α for various values of $\alpha=V_c/V_d$. I_p' has been obtained in each case by dividing I_p by its maximum value, which is given by Eq. (14A). From Eqs. (9A), (10A), and (11A), one obtains

$$\gamma/\alpha=(\Delta\nu/n\nu_R)/(\Delta\nu_c^*/n\nu_R), \tag{16A}$$

where $\Delta\nu_c^*/n\nu_R$ is the half width as defined by Eq. (10A) for a dee voltage V_c and arbitrary values of n and the detector probe position.

From Eq. (15A) it follows that the point P (Fig. 4) where the current goes to zero on the higher frequency side of resonance is given by $\gamma=(1-\alpha^2)^{\frac{1}{2}}$; therefore, according to Eq. (16A), one has at this point $\Delta\nu=\Delta\nu_c^*(\alpha^{-2}-1)^{\frac{1}{2}}$.

As explained in Sec. IV, the experimentally observed resonance curves of Fig. 9 have been plotted in terms of $\mu=(H/H')(n\nu_N/\nu)$ as the abscissa rather than in terms of $\Delta\nu$. If in Fig. 9 the value of μ at point P is designated by $(H/H')(n\nu_N/\nu)_P$, then in correspondence with the above value of $\Delta\nu$, we have

$$\Delta\mu=(H/H')[(\nu_N/\nu_R)-(n\nu_N/\nu)_P]$$
$$\cong(H/H')(\nu_N/\nu_R)(\Delta\nu_c^*/n\nu_R)(\alpha^{-2}-1)^{\frac{1}{2}},$$

from which we obtain:

$$(H/H')(n\nu_N/\nu)_P$$
$$\cong(H/H')(\nu_N/\nu_R)[1-(\Delta\nu_c^*/n\nu_R)(\alpha^{-2}-1)^{\frac{1}{2}}]. \tag{17A}$$

This equation has been plotted in Fig. 12.

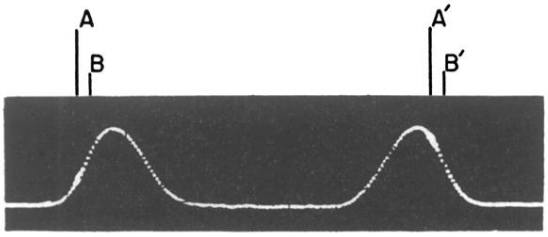

FIG. 8. Photograph of a typical cyclotron resonance trace at the 9th multiple of ν_R. The vertical deflection is proportional to the detector probe current; in the horizontal direction, the dee frequency first increases and then decreases, thus sweeping twice through resonance. The two bright spots on the trace at A and A′ are the frequency markers, which are slightly displaced from their true positions B and B′ because of time delay in the amplifiers. The relative width at half maximum amplitude is about 1/9000 for this resonance curve.